Sliding Mode Control for Position Tracking of Servo System with a Variable Loaded DC Motor

Akif Durdu, Emre Hasan Dursun
Robotics Automation Control Laboratory (RAC-LAB),
Department of Electrical & Electronics Engineering, Konya Technical University,
Konya, Turkey
adurdu@ktun.edu.tr

***Abstract*—In this paper, the real-time position control of servo system is carried out using sliding mode control (SMC) method based on variable structure control (VSC). As DC Motors are commonly used in many industrial applications and robotics, studies in this paper have are tested on a DC servo system, which is designed and produced by Quanser Inc. Three different types of sliding mode controllers are designed for position control of servo system and, later, performance comparison of DC Motor on Servo system is made. According to results obtained from real-time servo system, it is shown that SMC method is robust against to disturbing effects, variabilities, and uncertainties on the systems. Outstanding part of this paper is that designed controllers are implemented to servo system in real-time with a variable loaded DC Motor. Moreover, this study shows that this control structure can be performed as high performance in the real-time motor control applications.**

***Index Terms*—DC motor; Nonlinear control; Position control; Robust control; Servo system; Sliding mode control.**

I. INTRODUCTION

DC Motors are widely used in angular position control applications, which are often encountered in industry. They have certain characteristics, such as high efficiency, successful performance, and easy controllability. Thus, they are widely preferred in raw steel mills, electric winches, robotic manipulators and many industrial applications [1]–[3]. Precise position control constitutes a requirement in many servo motor applications, such as positioning of a robot arm from space research to a medical field [4]. In position control, motor's speed and position information, as well as performance of the controller, and accuracy of the controller and response time of the system are important.

In many industrial applications, where PID controllers are widely used, position control has created a major problem for many years [5]. Although PID controllers can be designed easily, they have several disadvantages about the robustness against system uncertainties and external disturbing effects. Also, they cannot be produced to get successful results in nonlinear control applications [4]. Even if a good performance characteristic can be obtained by classical PID parameters, when operating conditions change, an expected performance cannot be achieved by using PID controller with fixed parameters [6]. DC servo motor systems have usually uncertain and nonlinear characteristics, which effect the controller negatively. Therefore, the self-adjusting adaptive control or a robust control given rapid responses is needed [7].

Many different methods are proposed to control DC Motors and servo systems. These approaches are PID control, fractional order PID control [8], fuzzy logic control [9], linear quadratic regulator (LQR), PID control based on artificial intelligence [10], sliding mode control [11], and iterative learning control [12]. Moreover, studies on hybrid control methods continues.

Sliding mode control (SMC) method is one of nonlinear control techniques and has some attractive characteristics, such as quickly response, a good transient response, successful adaptation to disturbing effect, and insensibility to change of system parameters [6], [13]. SMC can be used for speed and position control of electric motors [6].

In this paper, position control of a servo system is carried out in real-time by using various types of SMC as a robust control method. Structures of SMC are designed in three different types, which are SMC, modified SMC (M-SMC), and SMC with a PID surface (PIDsur-SMC). All designed controllers are tested in real-time. As in the experimental studies various metallic weights are added to the system for extra loading, additionally, controller performances are relatively compared to each other by using certain error criteria.

This paper is organized as follows. Firstly, SMC method and its conventional theory are decribed in Section II. Then, information about servo system that is performed real-time application is given in Section III. Also, in Sec. IV, the implemented experimental studies and stages are referred. Testing steps and discussion are presented in Section V. According to loading condition and international performance criteria, comparisons are made in the section mentioned above as well. Lastly, results and recommendations are given in Section VI.

II. SLIDING MODE CONTROL

The theory of sliding mode control (SMC) is based on a variable structure control technique proposed in 1950, which have been attracting researchers studying control methods for 20 years already [14], [15]. SMC, which shows insensibility to system's parametric changes, disturbing

Manuscript received 20 November, 2018; accepted 28 June, 2019.

effects, and can operate under uncertain conditions, is a robust control method for linear and nonlinear systems [14], [16]. Thanks to these advantageous properties, SMC draws much interest in machine control applications [17]. Conventional SMC theory is composed of two phases, which are reaching mode and sliding mode as can be seen in Fig.1.

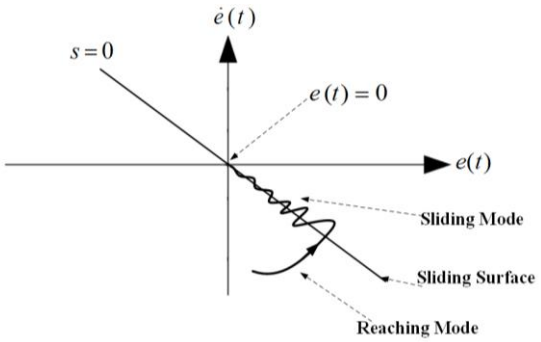

Fig 1. Phase portrait of SMC.

The most important step to design SMC is to create the sliding surface. High frequency switching control signal, which is demonstrated in Fig. 2, moves states of the system to a significant surface. Therefore, this surface is named as sliding surface. Movement on surface is described as sliding mode and movement up till reaching the surface represents the reaching mode [18].

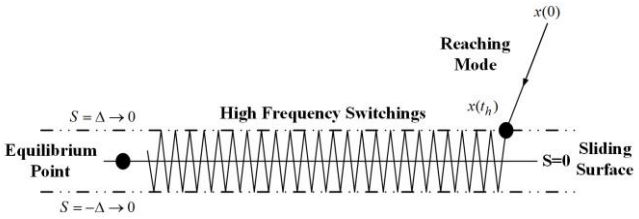

Fig. 2. Sliding surface, reaching mode, and high frequency switchings.

Main purpose of SMC is that system output arrive to desired system output. In other words, control signal $u(t)$, which tracking error converges to zero or keeps to minimal level, is to going to be produced. States of the system reaches to sliding surface by passing between stable and unstable trajectories and, then, tracking error converges to zero at minimal range on the sliding surface. However, chattering phenomenon occurs due to high frequency switchings.

SMC generates an increasing interest in robotics, aviation and space technologies, automotive industry, electric motor drives, and power converters and their controllers [1], [15], [16].

The first step to design the SMC is to form the mentioned sliding surface. The equation commonly used for the sliding surface is as follows

$$s(x,t)=\left(\frac{d}{dt}+\lambda\right)^{n-1}e(t). \tag{1}$$

It is shown that sliding surface is a function, which is related to tracking error, namely a difference between reference and measurement output. In here, *n* demonstrates the degree of the system and λ is a positive number that represents the slope of the sliding surface. Both sliding function and its derivative across the sliding surface is equal to zero as $s(t)=0$ and $\dot{s}(t)=0$.

Control law $u(t)$ that is purpose of the SMC consists of two parts as equivalent control signal $u_{eq}(t)$ and switching control signal $u_{sw}(t)$,which are shown below:

$$u(t)=u_{eq}(t)+u_{sw}(t), \tag{2}$$

$$u_{sw}(t)=K\,\mathrm{sgn}(s), \tag{3}$$

where *K* is a positive number, which is selected quite big to suppress system's uncertainties and unexpected dynamics, and *sgn(.)* presents signum function. Signal $u_{sw}(t)$ pulls states of the system to sliding surface while $s(t)\neq 0$. After reaching to sliding surface, switching control signal is switched off. Because of situation, although equivalent control signal is continuous, switching control signal is discontinuous. Block schema of conventional SMC is indicated in Fig. 3.

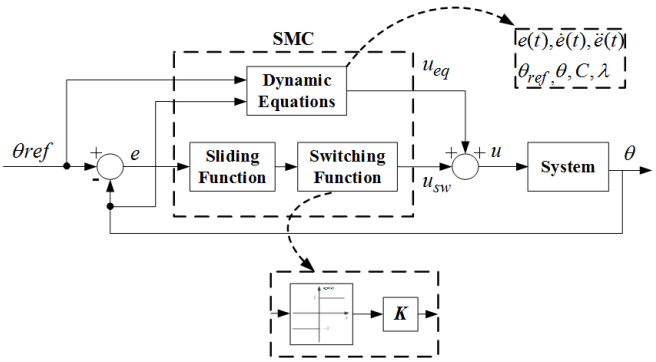

Fig. 3. Block schema of conventional SMC.

Lyapunov function, which is expressed as

$$V=\frac{1}{2}s^2, \tag{4}$$

is commonly used for sliding mode [19] and system stability law is obtained in (6) by using (5):

$$s\dot{s}<0 \quad \forall s\neq 0, \quad V(0)=0, \quad V(s)>0\ , \tag{5}$$

$$\dot{V}=\frac{1}{2}\frac{d}{dt}s^2\leq -\eta|s|, \tag{6}$$

where $s,\dot{s},\text{and}\,\eta$ are described as a sliding function, its derivative, and a constant, respectively.

When converge condition is described in (7), sliding mode condition is defined in (8):

$$s\dot{s}\leq -\eta|s|, \quad s\dot{s}\leq -\eta\,\mathrm{sgn}(s)s, \tag{7}$$

$$\dot{s}\,\mathrm{sgn}(s)\leq -\eta. \tag{8}$$

System arrives to sliding mode if condition $\eta>0$ is ensured.

Although conventional SMC has advantages, such as robustness, it has a disadvantage known as chattering phenomenon [20]. Chattering phenomenon emerge from

high frequency switchings and sharpness in signum function. Even if it's effects may not be seen much in the simulation studies, when real-time applications are carried out, it is understood that chattering phenomenon is a significant issue that needs to be considered. Too big control signals for actuators can cause problems in the real-time systems. Especially, it may cause breakdown or adverse effects, audible sounds, and heating of power circuits in the controlled mechanical systems [21], [22]. Additionally, when the real-time application is implemented, it cannot be achieved to infinitely fast switching assumption, which is basis of the general theory because of time delays and physical limitations [23].

In the literature, it is encountered with many different approaches to relieve the chattering phenomenon. For example, smoothing can be provided by changing of signum function or by using fuzzy logic. In fourth section of this paper, details are mentioned.

III. Model of the Servo Motor System

Permanent magnet DC Motors (PMDC) benefits for actuation. They are mentioned in former sections due to the fact that they are widely used in control systems in general. To express it in a simple way, Quanser SRV-02 is a rotary servo control system, which is designed for speed and position control of DC Motor. This servo system ensures a real-time design and enables different control algorithms to be tested.

The servo system consists of a DC Motor and a gearbox. The servo system can turn load and load arm via external gears. It has tachometer, potentiometer, and digital encoder to measure angular velocity and position [24]. Thanks to different selections, it offers the users an opportunity to work via both analogue and digital position measurements [24]. Moreover, there is a possibility of adding external modules to servo system. Equivalent scheme of the rotary servo system is demonstrated in Fig. 4. Specific parametric data for DC Motor, gearboxes, and the others is explained as in Table 1 [25], [26].

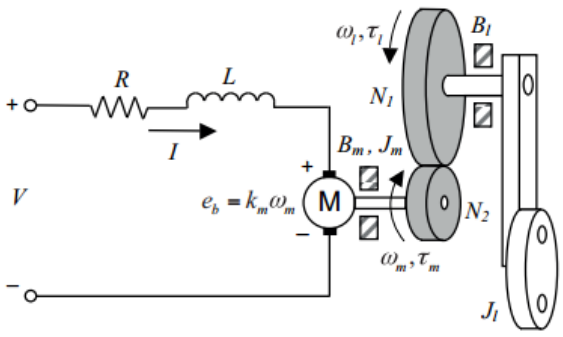

Fig. 4. Equivalent circuit of servo system.

For the system modelling (Fig. 4), electrical and mechanical equations are as shown in (9)–(16):

$$V(t) = R\,i(t) + L\frac{di(t)}{dt} + e_b(t), \tag{9}$$

$$\tau_m(t) = \tau_l + J_m\frac{d^2\theta_m(t)}{dt^2} + B_m\frac{d\theta_m(t)}{dt}, \tag{10}$$

$$\tau_m(t) = K_t\,i(t), \tag{11}$$

$$e_b(t) = K_m\,\omega_m(t) = K_m\frac{d\theta_m(t)}{dt}, \tag{12}$$

$$\dot{i}(t) = \frac{V(t)}{L} - \frac{K_b}{L}\omega(t) - \frac{R}{L}i(t), \tag{13}$$

$$T(t) = K_t\,i(t), \tag{14}$$

$$\theta_l = \frac{1}{N_g}\theta_m(t), \tag{15}$$

$$\tau_l(t) = \frac{1}{N_g\eta_g}\left(J_l\frac{d^2\theta_l(t)}{dt^2} + B_l\frac{d\theta_l(t)}{dt}\right), \tag{16}$$

where N_g signifies total gear ratio and η_g specifies gearbox efficiency. Equations for variable load torque are as in (15), (16). In here, θ_l and θ_m indicate the angle of load and armature, respectively.

In the next section, sliding mode controllers are designed by putting in places necessary coefficients and by using the equations mentioned above.

TABLE I. PARAMETERS OF SERVO SYSTEM.

Symbols	Explanation	Unit
V	Armature voltage	6 Volt
R	Armature resistance	2.6 Ohm
L	Armature inductance	0.18 mH
K_b	Back emf constant	0.00767 Vs/rad
K_t	Torque constant	0.00767 Nm/Amper
N_g	Gear ratio (N_2/N_1)	70
η_g	Gearbox efficiency	0.9
J_m	Inertia of motor	$4.6\,10^{-7}\,kg.m^2$
B_m	Viscous friction of motor	≅ 0
J_{L_in}	Initial load and inertia of gearbox	$4.83\,10^{-7}\,kg.m^2$
J_{L_sub}	Addition load and inertia of gearbox	$4.83\,10^{-6}\,kg.m^2$
B_{L_in}	Viscous friction with initial load	$4.41\,10^{-6}\,Nm/(rad/\sec)$
B_{L_sub}	Viscous friction with addition load	$3.41\,10^{-5}\,Nm/(rad/\sec)$
$e_b(t)$	Back emf	Volt
T_L	Load torque	Nm
T_e	Torque produced By motor	Nm
ω_m	Angular velocity	Rad/s
θ_m	Angular position	Rad

IV. Experimental Studies

Block schema of experimental servo system is shown in Fig. 5.

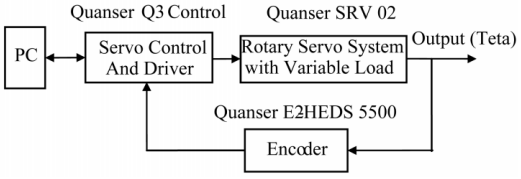

Fig. 5. Block schema of experimental system

In experimental study, a servo module, named as Quanser SRV-02, utilized digital signal processing is used. Practise image of rotary servo system used in this paper is indicated

in Fig. 6. In this figure, computer, servo control unit and driver, rotary servo system, initial loaded arm, addition loads, and the other environment components are exhibited. It has benefitted from a data acquisition card with amplifier named as Q3 Control PaQ-FW. Designed controllers are run computer aided and transferred to motor system via a software.

In this study, analyses are made by adding monitoring in different levels by means of addition loads. Thanks to using, firstly, an initial load and, later, for loading low and high weighted metallic objects, three types of loading conditions are performed and results are analysed.

Servo system can be modelled approximately as a first order system to actualize the speed control. Additionally, degree of the system for the position control is shown as a second order in [24], [25]. Transfer function of the servo system for angular velocity and angular position are described in (17), (18):

$$\frac{\omega(s)}{V(s)} = \frac{K}{\tau s + 1}, \tag{17}$$

$$\frac{\theta(s)}{V(s)} = \frac{K}{s(\tau s + 1)}, \tag{18}$$

where K and τ are defined as steady state gain of the system and time constant, respectively, and their values are as in (19), (20):

$$\frac{\omega(s)}{V(s)} = \frac{1.53}{0.0254 s + 1}, \tag{19}$$

$$\frac{\theta(s)}{V(s)} = \frac{1.53}{s(0.0254 s + 1)}. \tag{20}$$

If transfer function of the system converts to state-space model, it is obtained as follows:

$$\begin{bmatrix} \dot{\theta}(s) \\ \dot{\omega}(s) \end{bmatrix} = \begin{bmatrix} 0 & 1 \\ 0 & -1/\tau \end{bmatrix} \begin{bmatrix} \theta(s) \\ \omega(s) \end{bmatrix} + \begin{bmatrix} 0 \\ K/\tau \end{bmatrix} V(s), \tag{21}$$

$$y(s) = [1 \quad 0] \begin{bmatrix} \theta(s) \\ \omega(s) \end{bmatrix}. \tag{22}$$

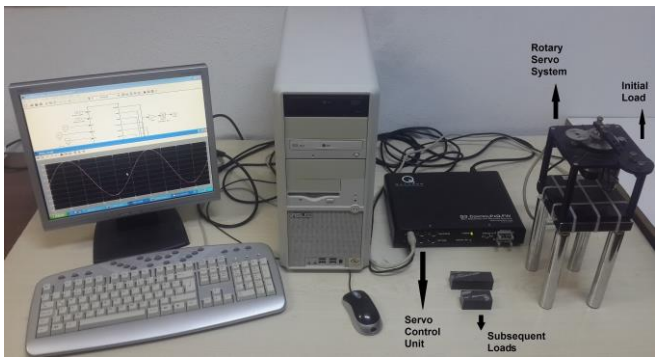

Fig. 6. Image of experimental system.

A. Theory 1 – Conventional SMC

In section II, the structure of conventional SMC is mentioned. Conventional SMC is a structure of control, which has a switching control signal with signum function as shown in (2), (3). Additionally, theoretical implementation of conventional SMC is expressed in this section.

The equation of state for a second order system is generally identified as

$$\dddot{X} = -A\ddot{X} - BX + Cu - D\tau - E\dot{\tau}, \tag{23}$$

where X is specified as a primary variable in equation of the state. Also, its first and second derivatives are $\dot{X}$ and $\ddot{X}$, control signal u, disturbing effect τ, such as friction and load changing, and its derivative $\dot{\tau}$ are described, respectively. Here, A, B, and C symbolize coefficients obtained from state equation of the system, while D and E express unknown variable coefficients of disturbing effect. If disturbing effects in (23) are combined with a single variable, which is named as H, finally, equation can be displayed as

$$\dddot{X} = -A\ddot{X} - BX + Cu + H. \tag{24}$$

In this study, equation of the state for position control of servo system can be created as in (25) by benefiting from (19), (20) which is a transfer function equation of the system

$$\dddot{\theta}(s) = -39.3701\ddot{\theta}(s) + 60.2362\, u + H. \tag{25}$$

While modelling in the nominal conditions, design and resolution are made as intended when disturbance effects is equal to zero. If dynamic states are analysed under condition $H = 0$, namely in the nominal conditions, it is obtained as

$$\dddot{\theta}(s) = -39.3701\ddot{\theta}(s) + 60.2362\, u. \tag{26}$$

For creating a generally form, variables A and C are used. Thus, a new equation form is turn into

$$\dddot{\theta}(s) = -A\ddot{\theta}(s) + C\, u, \qquad \{A = 39.3701, C = 60.2362\} \tag{27}$$

if variables are defined as:

$$y = \theta(s), \quad u = V(s), \tag{28}$$

$$\begin{cases} X_1 = e = \theta_{ref} - \theta_m, \\ X_2 = \dot{e} = \dot{X}_1 = \dot{\theta}_{ref} - \dot{\theta}_m, \\ \dot{X}_2 = \ddot{e} = \ddot{\theta}_{ref} - \ddot{\theta}_m, \end{cases} \tag{29}$$

where e, $\dot{e}$, and $\ddot{e}$ represents error and first and second derivatives of error, respectively. Besides, θ_{ref} and θ_m are defined as reference and measurement position variables. Sliding surface and its derivative can be defined as follows:

$$s = C X_1 + X_2 = C(\theta_{ref} - \theta_m) + (\dot{\theta}_{ref} - \dot{\theta}_m), \tag{30}$$

$$\dot{s} = C(\dot{\theta}_{ref} - \dot{\theta}_m) + (\ddot{\theta}_{ref} - \ddot{\theta}_m). \tag{31}$$

If the derivative of sliding surface is equal to zero as demonstrated in (30), which should be equal to switching control signal, and, later, if (31) is substituted in (32), derivation of the equation of sliding surface can be obtained

as in (33):

$$\dot{s} = -K\,\mathrm{sgn}(s), \tag{32}$$

$$\dot{s} = C\left(\dot{\theta}_{ref} - \dot{\theta}_m\right) + \left(\ddot{\theta}_{ref} - \ddot{\theta}_m\right) = -K\,\mathrm{sgn}(s). \tag{33}$$

If they are replaced in

$$C\dot{\theta}_{ref} + \ddot{\theta}_{ref} - C\dot{\theta}_m - \ddot{\theta}_m = -K\,\mathrm{sgn}(s), \tag{34}$$

which is expansion of (33), control signal u is produced as indicated below

$$u = \frac{1}{60.2362}\left[C\dot{\theta}_{ref} + \ddot{\theta}_{ref} + (39.3701 - C)\dot{\theta}_m + K\,\mathrm{sgn}(s)\right]. \tag{35}$$

In experimental study, parametric coefficients are determined as K=200 and C=70. When control signal u is being transferred, adaptation coefficient Γ is specified as 0.15, which can be seen below

$$u_{servo} = \Gamma * u. \tag{36}$$

B. Theory 2 – Modified SMC

Signum function, *sgn(s)*, generates discontinuous control on the sliding surface, and hence it generally produces chattering phenomenon in control input. When intended to chattering reduction, some modifications can be made and different function types can be used. In this step, a modification in the signum function is done and replaced a smooth transition nonlinear sigmoid function, which is indicated as follows

$$u_{sw}(t) = K\frac{s}{|s| + \delta}. \tag{37}$$

While $\forall\delta : \Re^+$ and δ is in the range of $0 < \delta < 1$. Moreover, it is a tuning parameter of the sigmoid function and δ is selected suitable for following of ideal performance.

Structure of control signal u produced by conventional SMC is converted to a form such that

$$u = \frac{1}{60.2362}\left[C\dot{\theta}_{ref} + \ddot{\theta}_{ref} + (39.3701 - C)\dot{\theta}_m + K\frac{s}{|s| + \delta}\right]. \tag{38}$$

In experimental application of modified SMC, parametric coefficients are adjusted as K=200, C=40, and δ=0.99. Furthermore, adaptation coefficient Γ is designated as 0.15.

C. Theory 3 – PIDsur-SMC

In this section of theory groups, sliding surface design for SMC is presented as with PID type surface [27], [28], which is displayed as

$$s = \lambda_1 e + \lambda_2 \int e + \lambda_3 \dot{e}. \tag{39}$$

If it is benefitted from (29) and the second derivative of error is replaced in (40), which is first derivative of sliding surface, and, then (40) is equal to zero, (41) is obtained

$$\dot{s} = \lambda_1 \dot{e} + \lambda_2 e + \lambda_3 \ddot{e}. \tag{40}$$

If state equation of system, which can be shown in (26), is substituted in (40), (41) is acquired. Therefore, equivalent control signal is defined as in (42) that edited version of equation:

$$\lambda_1 \dot{e} + \lambda_2 e + \lambda_3\left(\ddot{\theta}_{ref} + A\dot{\theta} - C\,u\right) = 0, \tag{41}$$

$$u_{eq} = \frac{1}{\lambda_3 C}\left[\lambda_1 \dot{e} + \lambda_2 e + \lambda_3 \ddot{\theta}_{ref} + \lambda_3 A\dot{\theta}\right]. \tag{42}$$

As it is indicated in

$$u(t) = u_{eq}(t) + u_{sw}(t), \tag{43}$$

main control signal for SMC composes of two parts, such as equivalent and switching control signal, which are also symbolized as u_{eq} and u_{sw}, respectively

Smooth saturation function [29] displayed as

$$u_{sw}(t) = K_{sw}.sat(\frac{s}{\varphi}), \tag{44}$$

is used for describing u_{sw} and, moreover, graph of this function is visualized in Fig. 7.

Parametric coefficients are selected as λ_1=70, λ_2=10, λ_3=0.6, $K_{sw} = 8$, and ϕ=5. Adaptation coefficient Γ is determined as 0.15, which is shown in (36).

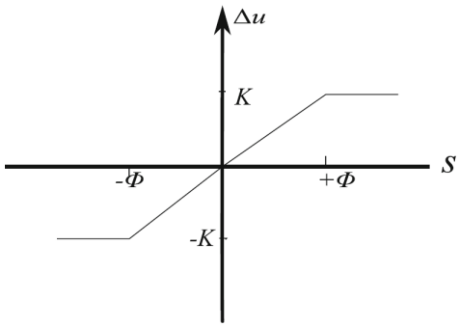

Fig. 7. Boundary layer graph of smooth saturation function.

D. Theory 4 – PID Control

PID control is a control algorithm, which has commonly been used since the 1940s. PID controllers are prevalently used in many different specific fields like robotics, unmanned aerial vehicles, chemical industry, steam production, oil processing, motor control, and automation systems.

PID controllers have a simple structure that consist of proportional, integral, and derivative parts. For adapting and determining behaviour of closed loop control system, these parameters should be adjusted effectively. Because of the PID control, successful performance is exhibited in many different processes and it is easy to design. This method is highly advantageous. There are uncertain and time varying system dynamics in many processes in industry. Because of

the classical PID controllers fixed parameters, they cannot display a good performance [7]. Thus, there is a need for a control structure that could cope with all situations mentioned above.

Time domain representation of PID controller is indicated as

$$u(t) = K_p e(t) + K_d \frac{de(t)}{dt} + K_i \int e(t)dt, \tag{45}$$

where $e(t)$ is error between input and output and, also, K_p, K_i, and K_d are expressed as proportional, integral, and derivative gain coefficients, respectively.

E. Performance Criteria

In control systems, some specific performance criteria, which are generally used to measure and compare system performance, are available. In this study, the evaluations are carried out for three different criteria: Integral Square Error (ISE), Integral Absolute Error (IAE), and Integral Time-weighted Absolute Error (ITAE). Therefore, calculation formulas of these criteria are expressed as follows:

$$ISE = \int e^2 dt, \tag{46}$$

$$IAE = \int |e| dt, \tag{47}$$

$$ITAE = \int t\ |e| dt. \tag{48}$$

V. Testing Steps and Discussion

By determining a sinusoidal reference for position tracking, response of the motor system is analysed according to this reference position. All graphs of performed position tracking for designed controllers are shown in Fig. 8. Experimental results are obtained by considering loading condition and by comparing performance in point of ISE, IAE, and ITAE criteria, which is explained as in Table II. As it is understood from the graphs, computing of performance criteria is done for 2.5 s that period of the reference signal. According to Table II, the best performance is produced by PIDsur-SMC for all loading conditions, and, later, M-SMC and SMC produces, respectively. In this study, generated graphs indicate response of system for the first 5 s.

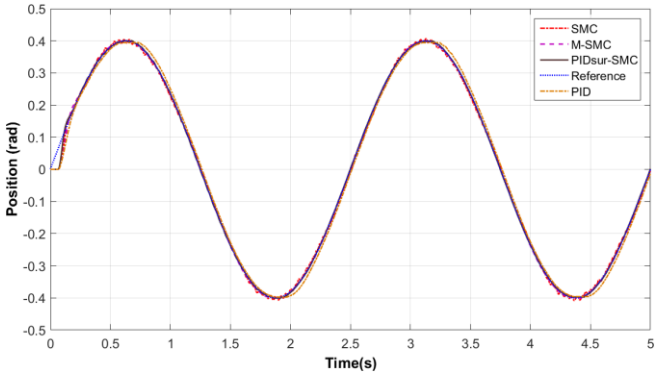

Fig. 8. Change of the position tracking under initial load.

In Figure 8, position-time graph of servo system for four type controllers under initial load is drawn. Because of data is close to each other, a zoomed image is demonstrated in Fig. 9. It can be seen that all three different SMC controllers actually produce quite successful results. However, if a comparison is made among them, PIDsur-SMC`s tracking trajectory is the nearest to reference position. However, PID controller has the worst tracking compared the others. Also, according to controllers, position error of servo system under initial load is demonstrated in Fig. 10. PIDsur-SMC can track the desired reference trajectory at least error. Additionally, the change of the sliding surface for three SMC structures under initial conditions are indicated in Fig. 11. The sliding surface interval of the PIDsur-SMC in Fig.11 is the narrowest and nearest interval on the zero axis. Considering the interval of sliding surface, it can be mentioned that the controller displays more succeeded results for the narrowest range $\pm\nabla s$. Moreover, the change of the control signal transferred to the system by different controllers under initial load is indicated in Fig. 12.

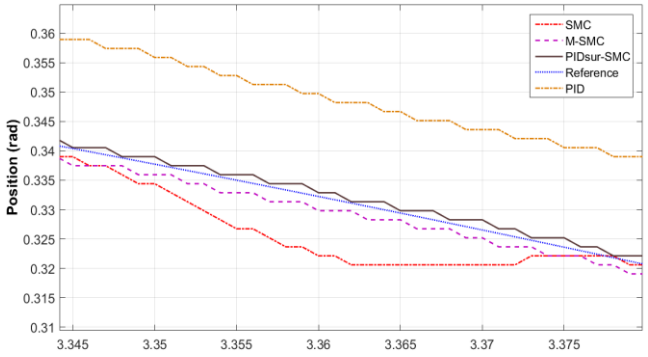

Fig. 9. Change of the zoomed position under initial load.

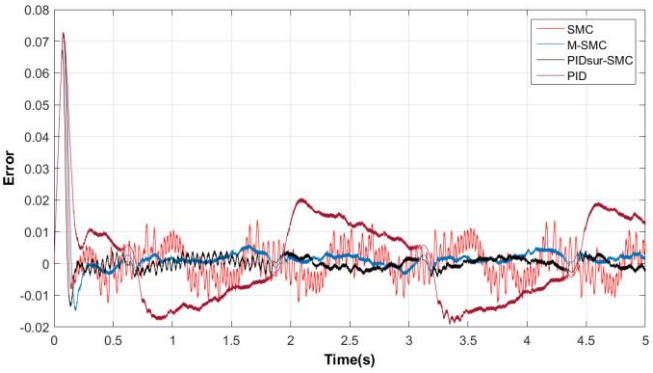

Fig. 10. Change of the error under initial load.

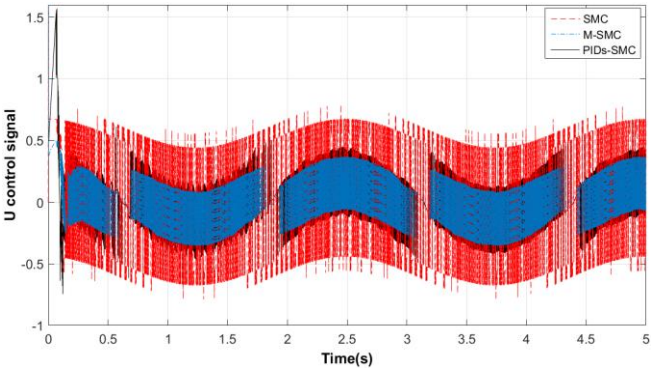

Fig. 11. Change of the control signal *u* under initial load.

Similarly, results for controllers under low load are demonstrated in Fig. 13–Fig. 16. When the changes of the error in Fig. 14 are analysed, amount of the error is at least in PIDsur-SMC. In conventional SMC, error changes in a wide range. It is demonstrated that error for PID control is

more than the other controllers. Increasing error amount means that position tracking has deteriorated. Moreover, in Fig. 16, it is shown how to change sliding surface for the controllers. Here, the nearest movement to sliding surface is performed by PIDsur-SMC, but sliding in conventional SMC is taken place in a large scale.

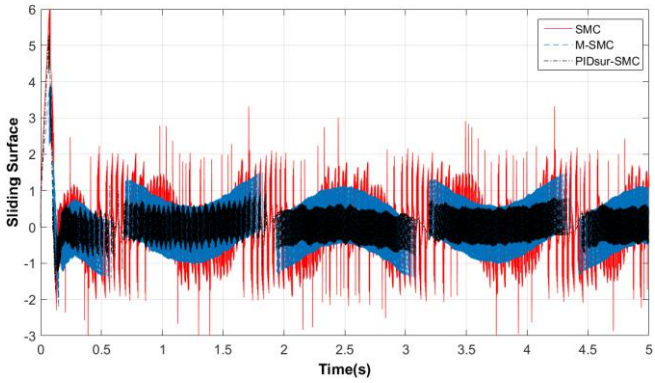

Fig. 12. Change of the sliding surface under initial load.

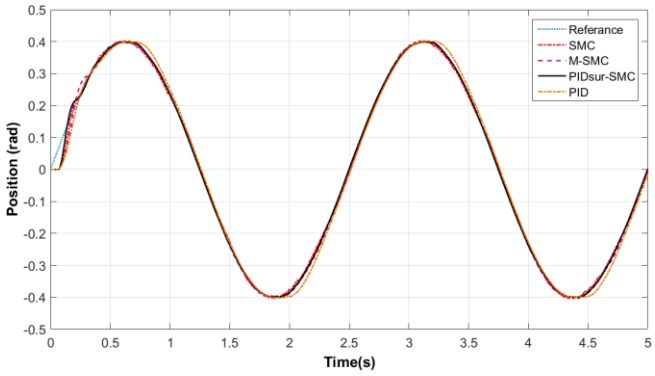

Fig. 13. Change of the position tracking under low load.

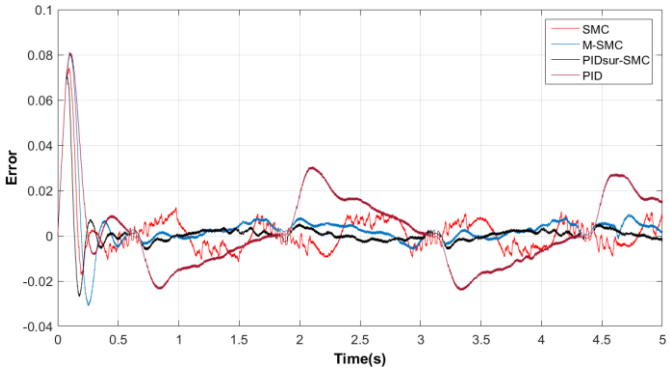

Fig. 14. Change of the error under low load.

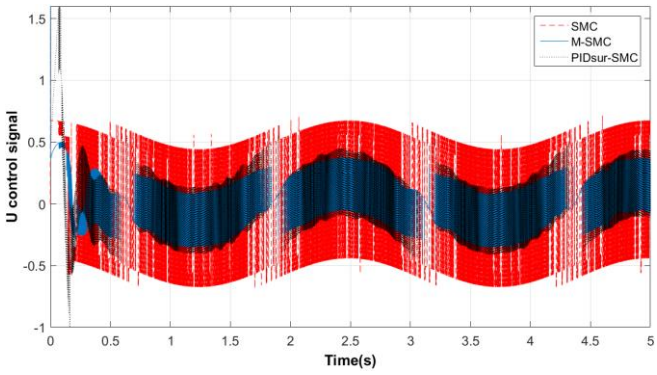

Fig. 15. Change of the control signal under low load.

In Figures 17–20, results of controllers under high load condition are indicated. It is observed that graphs are composed parallely with previous results. Especially, if changes of error and sliding surface are analysed, performance comparisons for controllers can be made. Thus, superiority rating for controllers can be made as PIDsur-SMC, M-SMC, and conventional SMC, respectively.

TABLE II. COMPARISONS OF CONTROLLERS.

Load	Criteria	PID	SMC	M-SMC	PIDsur-SMC
Initial	ISE	$35.72\ 10^{-5}$	$6.765\ 10^{-5}$	$1.108\ 10^{-5}$	$0.6535\ 10^{-5}$
Initial	IAE	0.02754	0.01072	0.004389	0.003481
Initial	ITAE	0.1053	0.04037	0.01702	0.01302
Low	ISE	$48.85\ 10^{-5}$	$7.289\ 10^{-5}$	$3.405\ 10^{-5}$	$1.005\ 10^{-5}$
Low	IAE	0.02886	0.01202	0.007467	0.004145
Low	ITAE	0.112	0.04408	0.03002	0.01531
High	ISE	$58.97\ 10^{-5}$	$8.755\ 10^{-5}$	$4.903\ 10^{-5}$	$1.506\ 10^{-5}$
High	IAE	0.03091	0.01323	0.008919	0.004861
High	ITAE	0.1205	0.04928	0.03626	0.01816

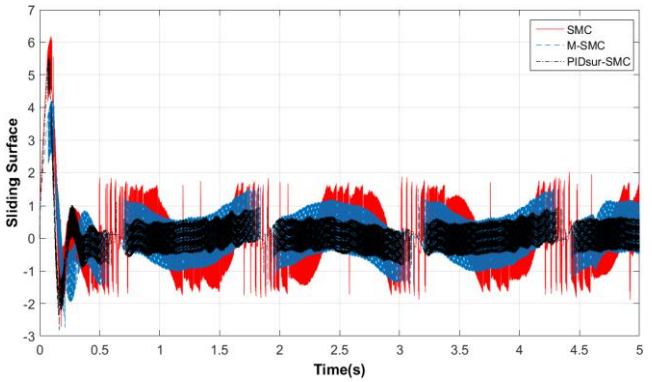

Fig. 16. Change of the sliding surface under low load.

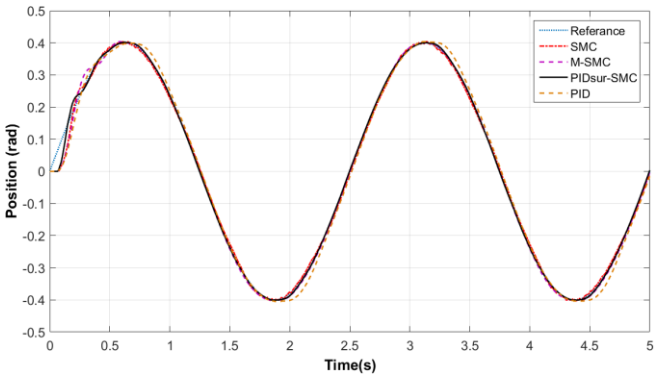

Fig. 17. Change of the position tracking under high load.

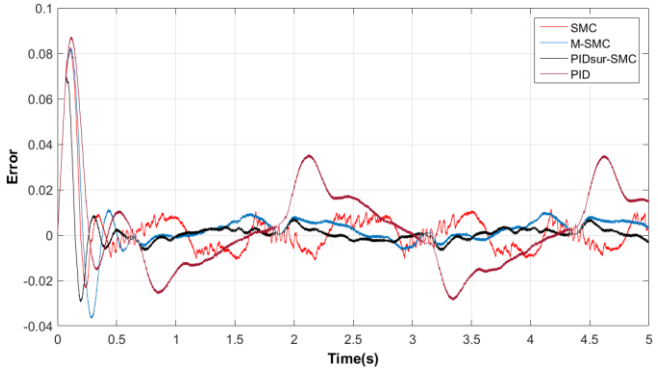

Fig. 18. Change of the error under high load.

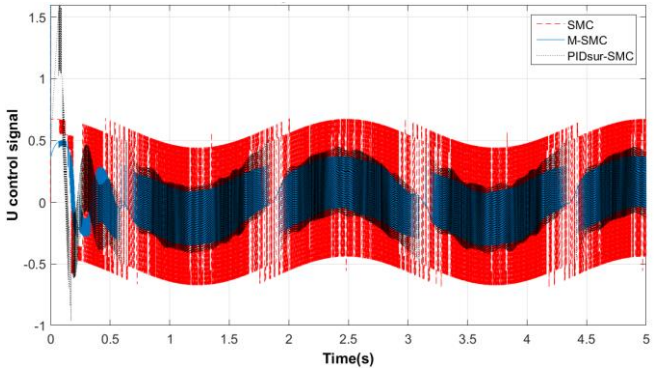

Fig. 19. Change of the control signal under high load.

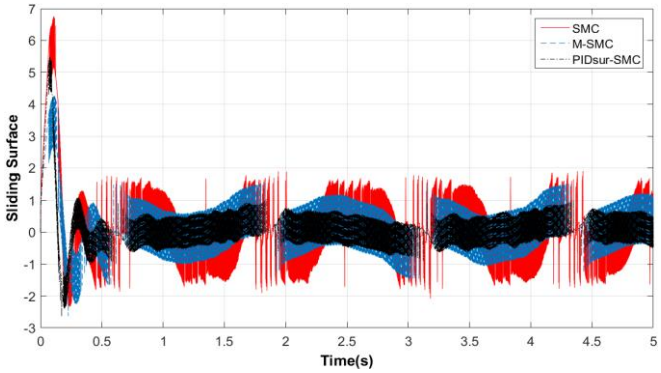

Fig. 20. Change of the sliding surface under high load.

VI. CONCLUSIONS

In this study, three different type sliding mode controllers are designed for position control of DC servo system, which is an extremely important issue in the control systems. Performance of controllers are compared after implementing designed controllers to DC servo system under different load conditions. Conventional SMC is a method that produces chattering phenomenon. M-SMC is designed by modifying switching function and it relieves greatly this problem. In addition, it gives better results when compared to previous control structure. In the last control structure, an alteration is made in sliding surface, which is the basic building block of SMC. It is understood that a controller running more stable and better performance is generated. In experimental results, although it is concluded that three methods can be run on system real-time, it is shown that M-SMC and PIDsur-SMC run more stable without vibration and error. In motor control application, elimination of vibration is so important due to the fact that it may cause deterioration of mechanical system. In sensitive running conditions as in some robotic applications, uncertainties, sudden changes, time-varying load changes and precise position tracking, application of SMC method provides many advantages.

ACKNOWLEDMENT

Authors are grateful to Selcuk University Scientific Research Projects Office, Academic Training Program and Rac-Lab (www.rac-lab.com) for providing this study.

CONFLICT OF INTEREST

The authors declare no conflict of interest.

REFERENCES

[1] M. K. Khan, “Design and application of second order sliding mode control algorithms”, Ph.D. dissertation, Department of Engineering, University of Leicester, 2003.

[2] D. Yulin, “The analysis and implement of PLC- based PI control for the permanent magnet DC motor”, in *Proc. 2nd International Conf. Communication Systems, Networks and Applications*, Hong Kong, 2010, pp. 448–451. DOI: 10.1109/ICCSNA.2010.5588973.

[3] T. R. Dil Kumar and S. J. Mija, “Design and performance evaluation of robust SMC schemes for speed control of DC motor”, in *Proc. International Conf. Advanced Communication Control and Computing Technologies*, Ramanathapuram, 2014, pp. 88-92. DOI: 10.1109/ICACCCT.2014.7019235.

[4] S. Kurode, B. Tamhane, Dharmveer, and P. Dixit, “Robust control with simultaneous state and disturbance estimation using sliding modes”, in *Proc. 12th International Workshop on Variable Structure Systems (VSS)*, Mumbai, Maharashtra, 2012, pp. 237–242. DOI: 10.1109/VSS.2012.6163508.

[5] A. A. Al Rawi, R. B. Ahmad, and H. H. Tahir, “Chatter-less sliding-mode controller for DC motor”, in *Proc. IEEE Student Conf. Research and Development*, Putrajaya, 2013, pp. 54–59. DOI: 10.1109/SCOReD.2013.7002540.

[6] A. K. Kadam, D. D. Ray, S. R. Shimjith, P. D. Shendge, and S. B. Phadke, “Time delay controller combined with sliding mode for DC motor position control: Experimental validation on Quanser QET”, in *Proc. International Conf. Power, Energy and Control*, Sri Rangalatchum Dindigul, 2013, pp. 449–453. DOI: 10.1109/ICPEC.2013.6527698.

[7] K. Nouri, R. Dhaouadi, and N. B. Braiek, “Adaptive control of a nonlinear dc motor drive using recurrent neural networks”, *Applied Soft Computing*, vol. 8, no. 1, pp. 371–382, 2008. DOI: 10.1016/j.asoc.2007.03.002.

[8] S. K. Gupta and P. Varshney, “Fractional fuzzy PID controller for speed control of DC motor”, in *Proc. 3rd International Conf. Advances in Computing and Communications*, Cochin, 2013, pp. 1–4. DOI: 10.1109/ICACC.2013.7.

[9] J. Velagic and A. Galijasevic, “Design of fuzzy logic control of permanent magnet DC motor under real constraints and disturbances”, in *Proc. 3rd International Conf. Control Applications & Intelligent Control*, Saint Petersburg, 2009, pp. 461–466. DOI: 10.1109/CCA.2009.5281099.

[10] E. Buzi and P. Marango, “A Comparison of conventional and nonconventional methods of DC motor speed control”, in *Proc. 15th IFAC Workshop on International Stability, Technology, and Culture*, vol. 46, no. 8, 2013, pp. 50–53. DOI: 10.3182/20130606-3-XK-4037.00054.

[11] E. H. Dursun and A. Durdu, “Speed control of a DC motor with variable load using sliding mode control”, *International Journal of Computer and Electrical Engineering*, vol. 8, no. 3, pp. 219–226, 2016. DOI: 10.17706/ijcee.2016.8.3.219-226.

[12] D. Kowalów, M. Patan, W. Paszke, and A. Romanek, “Sequential design for model calibration in iterative learning control of DC motor”, in *Proc. 20th International Conf. Methods and Models in Automation and Robotics*, Miedzyzdroje, 2015, pp. 794–799. DOI: 10.1109/MMAR.2015.7283977.

[13] J.-J. E. Slotine and W. Li, *Applied Nonlinear Control*. Englewood Cliffs, New Jersey, Prentice Hall, 1991.

[14] V. Utkin, “Variable structure systems with sliding modes”, *IEEE Transactions on Automatic Control*, vol. 22, no. 2, pp. 212–222, 1977. DOI: 10.1109/TAC.1977.1101446.

[15] C. Edwards and S. K. Spurgeon, *Sliding Mode Control: Theory and Applications*, Taylor & Francis, 1998. DOI: 10.1201/9781498701822.

[16] V. Utkin, J. Güldner, and J. Shi, *Sliding Mode Control in Electromechanical Systems*, Taylor & Francis, 1999.

[17] B. Soysal, “Real-time control of an automated guided vehicle using a continuous mode of sliding mode control”, *Turk J Elec Eng & Comp Sci*, vol. 22, pp. 1298—1306, 2014. DOI: 10.3906/elk-1211-130.

[18] J. Y. Hung, W. Gao and J,. C. Hung, “Variable structure control: A survey”, *IEEE Transactions on Industrial Electronics*, vol. 40, no. 1, pp. 2–22, 1993. DOI: 10.1109/41.184817.

[19] G. Monsees, “Discrete-Time Sliding Mode Control”, Ph.D. dissertation, Delft University of Technology, 2002. DOI: 10.23919/ECC.2001.7076437.

[20] I. Boiko, L. Fridman, R. Iriarte, A. Pisano, and E. Usai, “Parameter

tuning of second-order sliding mode controllers for linear plants with dynamic actuators", *Automatica*, vol. 42, no. 5, pp. 833–839, 2006. DOI: 10.1016/j.automatica.2006.01.009.

[21] A. Pisano, "Second Order Sliding Modes: Theory and Applications", Ph.D. dissertation, Dipartimento di Ingegneria Elettrica ed Elettronica, Universit´a degli Studi di Cagliari, 2000.

[22] H. Brandtstadter, "Sliding Mode Control of Electromechanical Systems", Ph.D. dissertation, Technische Universitat München, 2009.

[23] N. T. Tai and K. K. Ahn, "A RBF neural network sliding mode controller for SMA actuator", *International Journal of Control, Automation and Systems*, vol. 8, no. 6, pp. 1296–1305, 2010. DOI: 10.1007/s12555-010-0615-8.

[24] A. Brindha, S. Balamurugan, and P. Venkatesh, "Real time experiment to determine transfer function of Quanser servo plant", in *Proc. International Conf. Recent Advancements in Electrical, Electronics and Control Engineering*, Sivakasi, 2011, pp. 253–257. DOI: 10.1109/ICONRAEeCE.2011.6129731.

[25] *SRV02 Rotary Servo Base Unit Setup and Configuration*, Quanser, ed. Canada: Quanser Inc., 2011.

[26] Ö. Aydoğdu and Ö. Alkan, "Adaptive control of a time-varying rotary servo system using a fuzzy model reference learning controller with variable adaptation gain", *Turk J Elec Eng & Comp Sci*, vol. 21, pp. 2168–2180, 2013. DOI: 10.3906/elk-1201-115.

[27] İ. Eker and Ş. A. Akınal, "Sliding mode control with integral augmented sliding surface: Design and experimental application to an electromechanical system", *Electrical Engineering*, vol. 90, no. 3, pp. 189–197, 2008. DOI: 10.1007/s00202-007-0073-3.

[28] Y. Li and Q. Xu, "Adaptive sliding mode control with perturbation estimation and PID sliding surface for motion tracking of a piezo-driven micromanipulator", *IEEE Transactions on Control Systems Technology*, vol. 18, no. 4, pp. 798–810, 2010. DOI: 10.1109/TCST.2009.2028878.

[29] R. M. Nagarale and B. M. Patre, "Exponential function based fuzzy sliding mode control of uncertain nonlinear systems", *International Journal of Dynamics and Control*, vol. 4, no. 1, pp. 67–75, 2016. DOI: 10.1007/s40435-014-0117-2.